Inorg. Chem. **2007**, *46*, 10252–10260

Synthesis, Structures, and Optical Properties of Cadmium Iodide/Phenethylamine Hybrid Materials with Controlled Structures and Emissions

Wei Wang,[†] Juan Qiao,*[,†,‡] Liduo Wang,[†] Lian Duan,[†] Deqiang Zhang,[†] Weitao Yang,[‡] and Yong Qiu*[,†]

Key Lab of Organic Optoelectronics & Molecular Engineering of Ministry of Education, Department of Chemistry, Tsinghua University, Beijing 100084, People's Republic of China, and Department of Chemistry, Duke University, Durham, North Carolina 27708-0354

Received April 17, 2007

A new type of organic–inorganic hybrid materials based on cadmium iodide (CdI_2) and phenethylamine (PEA) has been synthesized and characterized. The reaction of CdI_2 with PEA in a 1:2 molar ratio yields a four-coordinate hybrid material $CdI_2(PEA)_2$ (**1**) with extended 1D $(CdI_2)_n$ chains, while the reaction of CdI_2 with PEA in a 1:4 molar ratio produces a six-coordinate hybrid material $CdI_2(PEA)_4$ (**2**) with a discrete linear structure of CdI_2 moiety. By introducing a trace amount of Na_2S to the reaction for $CdI_2(PEA)_2$, we obtained a new compound $[CdI_2(PEA)_2]$-$(CdS)_{0.038}$ (**3**) with uniformly doped CdS nanoparticles. Steady and transient photoluminescence studies reveal that compounds **1** and **2** exhibit bright blue (465 nm) and green (512 nm) fluorescent emissions in solid state at room temperature, respectively, while compound **3** gives a broad and complex emission ranging from 450 to 700 nm. Theoretical studies of electronic structures were carried out using density functional theory in order to gain a good understanding of the luminescent behaviors of these hybrid materials.

Introduction

Organic−inorganic hybrid materials of metal halide/amine systems such as $MX_2(L)_n$ (M = Zn, Cd, Cu, Co, Fe, etc.; X = Cl, Br, I; L = organic ligands containing one or more N atoms as the coordination atoms; $n = 1, 2$) have been widely studied due to their interesting crystal structures and potential applications as photoactive materials.[1−3] Group 12 (IIB) metal halides are regarded to be particularly promising, due to the variety of coordination numbers and geometries provided by the d^{10} configuration of the metal centers. This structural diversity is closely dependent on factors such as the dimension of the metal ions and halides, nature of ligands, and the availability of other structure controlling interactions, such as hydrogen bonding and charge transfer. The structure diversity is particularly evident in cadmium(II) halide complexes from 0D,[4] 1D,[5−6] to 2D[7] by choosing proper organic and inorganic portions. Complexes of CdX_2L_2 (X = Cl, Br, and I; L = pyridine or similar small, monodentate ligands) typically form extended chain structures with the metal center in six-coordinate pseudo-octahedral coordination or four-coordinate tetrahedral coordination.[8] Recently, a family of cadmium halide/pseudohalide bpy (bpy = 2,2′-bipyridine or 4,4′-bipyridine) compounds have been synthesized and characterized.[9] These compounds show interesting structural modes and potential applications in organic optoelectronics. Optical properties of CdI_2(bpy) and ZnI_2(bpy) have also been investigated as these materials are fluorescent and might be used for electroluminescent (EL) devices.

In our work, we report novel CdI_2 based hybrid materials with phenethylamine (PEA) as the organic ligand. We choose

* To whom correspondence should be addressed. Fax: (+86)-10-62795137. E-mail: qiuy@mail.tsinghua.edu.cn (Y.Q.), qjuan@mail.tsinghua.edu.cn (J.Q.).
† Tsinghua University.
‡ Duke University.

(1) Bailey, R. D.; Hook, L. L.; Powers, A. K.; Hanks, T. W.; Pennington, W. T. *Cryst. Eng.* **1998**, *1*, 51.
(2) Handley, D. A.; Hitchcock, P. B.; Lee, T. H.; Leigh, G. J. *Inorg. Chim. Acta* **2001**, *314*, 14.
(3) Zhai, Q.; Wu, X.; Chen, S.; Lu, C.; Yang, W. *Cryst. Growth Des.* **2006**, *6*, 2126.
(4) Ni, J.; Xie, Y.; Liu, X.; Liu, Q. *Appl. Organomet. Chem.* **2003**, *17*, 315.
(5) Matsuda, K.; Shinkai, Y.; Irie, M. *Inorg. Chem.* **2004**, *43*, 3774.
(6) Seitz, M.; Kaiser, A.; Stempfhuber, S.; Zabel, M.; Reiser, O. *J. Am. Chem. Soc.* **2004**, *126*, 11426.
(7) Bailey, R. D.; Pennington, W. T. *Polyhedron* **1997**, *16*, 417.
(8) Hu, C.; Li, Q.; Englert, U. *CrystEngComm* **2003**, *5*, 519.
(9) Chen, W.; Wang, M.; Liu, X.; Guo, G.; Huang, J. *Cryst. Growth Des.* **2006**, *6*, 2289.

10.1021/ic7007304 CCC: $37.00
Published on Web 11/01/2007

PEA as the ligand because the hybrids containing PEA are luminescent and easily dissolved in organic solvents such as methanol and ethanol. It was found that the inorganic frameworks in the hybrids can be tuned from $(CdI_2)_n$ chains (1D) to CdI_2 dot (0D) just by changing the molar ratio of PEA and CdI_2 in the reaction mixture. Herein, we describe the synthesis and characteristics of $CdI_2(PEA)_2$ (**1**) and $CdI_2(PEA)_4$ (**2**). Compound **1** has a linear crystal structure with tetrahedral coordination of the metal center such as previously reported hybrid materials,[1,8,10] while compound **2** has a pseudo-octahedral coordination with discrete CdI_2 moieties which are surrounded by four PEA molecules. We have also measured the absorption and photoluminescence of the compounds and found that compound **1** exhibits blue fluorescence while compound **2** gives green fluorescence at room temperature. By doping a very small amount of CdS into compound **1,** a new compound of CdS-doped $CdI_2(PEA)_2$ (**3**) was obtained which exhibits orange fluorescence at room temperature. Molecular orbital calculations of ground and excited electronic states were carried out in combination of transient photoluminescence to understand the emission mechanism of these hybrids.

Experimental Section

Measurements. All of the chemicals are readily available from commercial sources and were used without further purification. Phenethylamine (99.5%) was purchased from Acros Organics, CdI_2 (99.5%) was from Beijing Chemical Reagents Co., and $Na_2S{\cdot}9H_2O$ (98%) was from Beijing Modern Eastern Fine Chemical. C, H, and N analyses were carried out with an Exeter Analytical CE-440 elemental analyzer. S analysis was carried out with an X-ray fluorescence spectrometer (XRF-1700). Na analysis was carried out with a Vista-MPX inductive coupled plasma atomic emission spectrometer (ICP-AES). The infrared spectra (KBr pellet) were recorded on a Perkin-Elmer spectrum GX FT-IR spectrophotometer over the frequency range of 400−4000 cm^{-1}. The SEM (scanning electron microscope) image was recorded on a Hitachi S-4500 scanning electron microscope using an accelerating voltage of 15 kV. High-resolution transmission electron microscopy investigations were carried out with a JEOL-2011 instrument. Thermal gravimetric analyses were performed on a TGA2050 of TA Instrument Corp. The diffuse reflection absorption spectra were recorded on a Hitachi U-3010 spectrophotometer equipped with an integrating sphere at room temperature (298 K). The absorption spectra were calculated by the Kubelka−Munk function:[11] $\alpha/S = (1 - R)^2/2R$, where α is the absorption coefficient, S is the scattering coefficient, which is practically wavelength independent when the particle size is larger than 5 μm, and R is the reflectance. Photoluminescence (PL) spectra were recorded at room temperature (298 K) on a Jobin Yvon FluoroMax-3 spectrofluorometer using a xenon arc lamp as the light source. The time-resolved fluorescence decays were measured with a time correlated single photon counting (TCSPC) system on Edinburgh Instruments (FLS920) and analyzed by the software provided by the supplier.

Syntheses. (a) $CdI_2(PEA)_2$ (1). CdI_2 (2.89 g, 7.89 mmol) and PEA (2 mL, 15.78 mmol) were dissolved in 20 mL of anhydrous methanol, respectively. Then the PEA/methanol solution was dropped into the CdI_2/methanol solution in a three-necked flask under magnetic stirring. The mixed solution was heated to reflux for 1 h and filtrated immediately. The hot filtrate was cooled to room temperature to obtain 2.33 g of needle crystals which were filtered again and dried in vacuo. Yield: 48.6% (based on cadmium iodide). Chemical analysis of the product $CdI_2(PEA)_2$ yielded the following. Calcd: C, 31.58; H, 3.64; N, 4.60. Found: C, 31.64; H, 3.62; N, 4.59. IR peaks (KBr, cm^{-1}): 3431 (m), 3307 (w), 3227 (s), 3139 (w), 2937 (w), 2880 (w), 1581 (s), 1498 (s), 1455 (s), 985 (s), 750 (s), 700 (s), 500 (m). Slow evaporation of the second time filtrate for 3 days yielded colorless, rectangle crystals which were suitable for X-ray measurement.

(b) $CdI_2(PEA)_4$ (2). A 1.24 g amount of compound **2** was prepared with CdI_2 (1.44 g, 3.95 mmol) and PEA (2 mL, 15.78 mmol) by a method similar to that described above for **1**. Note, the CdI_2/methanol solution was inversely dropped into the PEA/methanol solution and the cooling process of the hot filtrate was very slow; otherwise only compound **1** was obtained. Yield: 35.8% (based on cadmium iodide). Chemical analysis of the product $CdI_2(PEA)_4$ yielded the following. Calcd: C, 45.17; H, 5.21; N, 6.58. Found: C, 45.27; H, 5.11; N, 6.56. IR peaks (KBr, cm^{-1}): 3433 (m), 3323 (s), 3240 (w), 3150 (w), 2933 (w), 2875 (w), 1595 (s), 1487 (s), 1451 (s), 970 (s), 748 (s), 702 (s), 544 (m). Slow evaporation of the second time filtrate for 3 days yielded yellow, transparent, hexagon crystals which were suitable for X-ray measurement.

(c) CdS-Doped $CdI_2(PEA)_2$ (3). Compound **3** was prepared by introducing trace Na_2S in the PEA solution. $Na_2S{\cdot}9H_2O$ (0.038 g, 0.16 mmol) and PEA (1 mL, 7.89 mmol) were dissolved together in 10 mL of anhydrous methanol and CdI_2 (1.44 g, 3.95 mmol) in another 10 mL of anhydrous methanol. The former solution was added to the latter one, and the mixed solution was heated to reflux for 1 h and filtered immediately. The filtrate was kept in the refrigerator (4 °C) for 1 day and yielded light yellow, transparent, needle crystals which were suitable for X-ray measurement. Yield: 50.9% (based on cadmium iodide). Chemical analysis of compound **3** yielded C, 31.52; H, 3.66; N, 4.55; S, 0.2. ICP-AES analysis revealed the content of Na is lower than the limit of detection (1 ppm). As a result, the formula of compound **3** can be expressed as $[CdI_2(PEA)_2](CdS)_{0.038}$. IR peaks (KBr, cm^{-1}): 3430 (m), 3240 (s), 3289 (w), 3238 (w), 2939 (w), 2877 (w), 1580 (s), 1497 (s), 1458 (s), 992 (s), 752 (s), 695 (s), 504 (s).

X-ray Crystallography. The crystals of compounds **1**−**3** with the approximate dimensions of 0.02 × 0.2 × 0.6, 0.15 × 0.2 × 0.3, and 0.2 × 0.2 × 0.7 mm^3, respectively, were selected under a microscope and attached to the end of a quartz fiber. The room temperature (294 ± 1 K) single-crystal X-ray experiments were performed on a Bruker P4 diffractometer equipped with graphite-monochromatized Mo Kα radiation (λ = 0.710 73 Å) using the ω scan technique. Direct phase determination yielded the positions of Cd, I, N, and most of the C atoms. The remaining atoms were located in successive-difference Fourier syntheses. Hydrogen atoms were generated theoretically and rode on their parent atoms in the final refinement. All non-hydrogen atoms were subjected to anisotropic refinement. The structural solutions and refinements were performed using the SHELXTL NT v 5.10 program package (Bruker, 1997).[12] A summary of the refinement details and the resulting factors are given in Table 1.

Calculation Details. Calculations on the ground and excited electronic states of compounds **1**−**3** (omit the CdS dopant) were

(10) Altun, A.; Golcuk, K.; Kumru, M. *Vib. Spectrosc.* **2003**, *33*, 63.
(11) Kortüm, G. *Reflectance Spectroscopy*; Springer-Verlag: Berlin, Heidelberg, Germany, 1969.
(12) Sheldrick, G. M. *SHELXTL*, version 5.1; Bruker Analytical X-ray System: Madison, WI, 1997.

Table 1. Crystallographic Data for Compounds **1** and **2** and the $CdI_2(PEA)_2$ Matrix of Compound **3**

param	**1**	**2**	$CdI_2(PEA)_2$ matrix of compd **3**
empirical formula	$C_{16}H_{22}N_2CdI_2$	$C_{32}H_{44}N_4CdI_2$	$C_{16}H_{22}N_2CdI_2$
mol mass	608.58	850.94	608.58
color	colorless	yellow	light yellow
cryst syst	monoclinic	monoclinic	monoclinic
space group	*C*2/*c*	*C*2/*c*	*C*2/*c*
a, Å	33.349(5)	31.424(2)	29.832(3)
b, Å	4.846(1)	12.483(1)	5.137(1)
c, Å	13.075(2)	8.991(1)	27.674(3)
β, deg	105.65(1)	96.043(1)	111.04(1)
V, Å^3	2034.7(5)	3507.4(4)	3958.2(6)
Z	4	4	8
d_{calcd}, g cm^{-3}	1.987	1.611	2.042
abs coeff (μ), mm^{-1}	4.104	2.249	4.219
R_{int}	0.0418	0.0253	0.0295
R1, wR2 [$I \geq 2\sigma(I)$][a]	0.0424, 0.1069	0.0408, 0.0994	0.0499, 0.1390
R1, wR2 (all data)[a]	0.0466, 0.1104	0.0499, 0.1065	0.0755, 0.1534

[a] R1 = $\Sigma||F_o|$ EnDash $|F_c||/\Sigma|F_o|$; wR2 = $[\Sigma w(F_o^2 - F_c^2)^2/\Sigma(F_o^2)^2]^{1/2}$.

carried out using density functional theory (DFT) and time-dependent DFT (TD-DFT) at the B3LYP level.[13−14] "Double-ξ" quality basis sets were employed for the C, H, and N (6-31G*) and the Cd, I (LANL2DZ). The initial ground-state geometries were directly obtained from the X-ray crystal structures. The geometries were fully optimized with C_1 symmetry constraints. All calculations were performed with Gaussian 03 software package using a spin-restricted formalism.[15] The electron density diagrams of molecular orbitals were obtained with the ChemOffice 2002 graphics program.

Results and Discussion

Crystal Structures. The molecular structures of compounds **1**−**3** were elucidated by X-ray crystallography. The crystal data and selected bond lengths and angles are listed in Tables 1 and 2, respectively. The perspective drawings of the structures are shown in Figure 1 and the molecular packings of the crystal structures are shown in Figures 2, 3, and 5. The complexes with group 12 metal elements (Zn, Cd, and Hg) as the centered atom have different coordinate numbers from 4 to 8 due to the d^{10} configurations, and the structures of the complexes are diversified.[16] The coordinate number of this kind of organic−inorganic hybrid materials can be 4,[8] 5,[3] or 6,[7−9] depending on the organic ligand.

$CdI_2(PEA)_2$ (1). Compound **1** crystallizes in monoclinic space group with centric *C*2/*c* symmetry. The molecule has a monomeric structure with pseudo-tetrahedral coordination about the cadmium atom, which is quite different from the octahedrally coordinated $CdI_2(pyridine)_2$[1] and $CdI_2(pyrazine)$.[7] The lower coordination number allows a closer approach of the ligands to the metal center. The bond length of Cd1−N1 and Cd1−I1 is 2.246 and 2.771 Å, respectively. The complex also consists of infinite CdI_2-based chains, not being doubly bridged by the two iodine atoms. The extended CdI_2 chains are kept by intermolecular hydrogen bonding of N−H···I and $\pi-\pi$ stacking of the organic ligands (as shown in Figure 2a). The hydrogen bonding in single CdI_2 chain is moderate with the bond length of H1ba···I1 (x, $y-1$, z) of 2.946 Å, comparing with the van der Waals radii of H (1.06 Å) and I (1.98 Å).[17] The organic ligands (PEA) are well-arranged via $\pi-\pi$ stacking interaction (3.537 Å). Moreover, there is a weak Cd−I···Cd interaction (3.897 Å) between the adjacent CdI_2 due to the d^{10} configuration of Cd atom. The distance of adjacent Cd atom is 4.846 Å, and more details of the packing of CdI_2 in compound **1** are shown in Figure S1 of the Supporting Information. The chains are linked together by intermolecular hydrogen bonding of N1a−H1aa···I1 (x, $-y$, $z+1/2$) with the bond length of 3.050 Å (shown in Figure 2b). More information of the hydrogen bonding can be found in Table S1 of the Supporting Information.

Table 2. Selected Bond Lengths (Å) and Angles (deg) for Compounds **1** and **2**[a] and the $CdI_2(PEA)_2$ Matrix of Compound **3**

	Compound **1**		
C(1)−C(2)	1.401(1)	C(8)−N(1)	1.480(5)
Cd(1)−N(1)	2.246(3)	Cd(1)−I(1)	2.771(1)
C(1)−C(2)−C(3)	120.9(1)	N(1)−C(8)−C(7)	112.9(4)
N(1)−Cd(1)−N(1)^1	129.1(2)	N(1)−Cd(1)−I(1)^1	102.1(1)
N(1)−Cd(1)−I(1)	107.6(1)	I(1)^1−Cd(1)−I(1)	107.0(1)
	Compound **2**		
C(3)−C(4)	1.394 (4)	C(1)−N(2)	1.472 (3)
C(11)−C(12)	1.392 (5)	C(9)−N(1)	1.461 (3)
Cd(1)−N(1)	2.393(2)	Cd(1)−N(2)	2.372 (2)
Cd(1)−I(1)^2	3.030 (1)	Cd(1)−I(1)	3.030 (1)
I(1)−Cd(1)−I(1)^2	180.0 (0)	N(1)−Cd(1)−N(1)^2	180.0 (0)
N(2)−Cd(1)−N(2)^2	180.0 (0)	I(1)−Cd(1)−N(1)	94.9 (1)
I(1)−Cd(1)−N(2)	87.4 (2)	N(1)−Cd(1)−N(2)	91.7 (2)
	$CdI_2(PEA)_2$ Matrix of Compound **3**		
C(1)−C(2)	1.374 (9)	C(8)−N(1)	1.451 (8)
C(9)−C(10)	1.373 (1)	C(16)−N(2)	1.477 (6)
Cd(1)−N(1)	2.244 (5)	Cd(1)−N(2)	2.247 (4)
Cd(1)−I(1)	2.762 (1)	Cd(1)−I(2)	2.739 (1)
C(1)−C(2)−C(3)	121.1 (7)	N(1)−C(8)−C(7)	110.1 (6)
C(9)−C(10)−C(11)	121.6 (6)	N(2)−C(16)−C(15)	114.3 (4)
N(1)−Cd(1)−N(2)	116.2 (2)	N(1)−Cd(1)−I(2)	110.4 (1)
N(2)−Cd(1)−I(2)	108.7 (1)	N(1)−Cd(1)−I(1)	104.3 (1)
I(2)−Cd(1)−I(1)	112.2 (1)	C(16)−N(2)−Cd(1)	116.1 (3)

[a] Symmetry transformations used to generate equivalent atoms: (1) compound **1**, $-x+2$, y, $-z+3/2$; (2) compound **2**, $-x+3/2$, $-y+3/2$, $-z$.

$CdI_2(PEA)_4$ (2). Compound **2** has a nomomeric structure with octahedral coordination about the cadmium atom, which is quite different from compound **1**. To our best knowledge, Cd(γ-picoline)$_4$I$_2$[18] and [CdI_2(pyridine)$_4$](pyridine)$_2$[19] were hitherto reported as monomeric six-coordinate compounds of group 12 metal halide/organic ligand systems. Moreover,

(13) Becke, A. D. *J. Chem. Phys.* **1993**, *98*, 5648.
(14) Lee, C.; Yang, W.; Parr, R. G. *Phys. Rev. B* **1988**, *37*, 785.
(15) Frisch, M. J.; Trucks, G. W.; Schlegel, H. B.; Scuseria, G. E.; Robb, M. A.; Cheeseman, J. R.; Zakrzewski, V. G.; Montgomery, J. A.; Stratmann, R. E.; Burant, J. C.; Dapprich, S.; Millam, J. M.; Daniels, A. D.; Kudin, K. N.; Strain, M. C.; Farkas, O.; Tomasi, J.; Barone, V.; Cossi, M.; Cammi, R.; Mennuci, B.; Pomelli, C.; Adamo, C.; Clifford, S.; Ochterski, J.; Petersson, G. A.; Ayala, P. Y.; Cui, Q.;Morokuma, K.; Malick, D. K.; Rabuck, A. D.; Raghavachari, K.; Foresman, J. B.; Cioslowski, J.; Oritz, J. V.; Stefanov, B. B.; Liu, G.; Liashenko, A.; Piskorz, P.; Komaromi, I.; Gomperts, R.; Martin, R. L.; Fox, D. J.; Keith, T.; Al-Laham, M. A.; Peng, C. Y.; Nanayakkara, A.; Gonzalez, C.; Challacombe, M.; Gill, P. M. W.; Johnson, B. G.; Chen, W.; Wong, M. W.; Andres, J. L.; Head-Gordon, M.; Replogle, E. S.; Pople, J. A. *GAUSSIAN03*, revision C.02; Gaussian: Pittsburgh, PA, 2003.
(16) Shriver, D. F.; Atkins, P. W. *Inorganic Chemistry*; Oxford University Press: Oxford, U.K., 2006.
(17) Zhang, M. B.; Zhao, D. X.; Yang, Z. Z. *J. Theor. Comput. Chem.* **2005**, *4*, 281.
(18) Liptay, G.; Borbély-Kuszmann, A.; Wadsten, T.; Losonczi, J. *Thermochim. Acta* **1988**, *133*, 353.
(19) Ito, M.; Shibata, T.; Saito, Y. *Acta Crystallogr., Sect. C: Cryst. Struct. Commun.* **1984**, *40*, 2041.

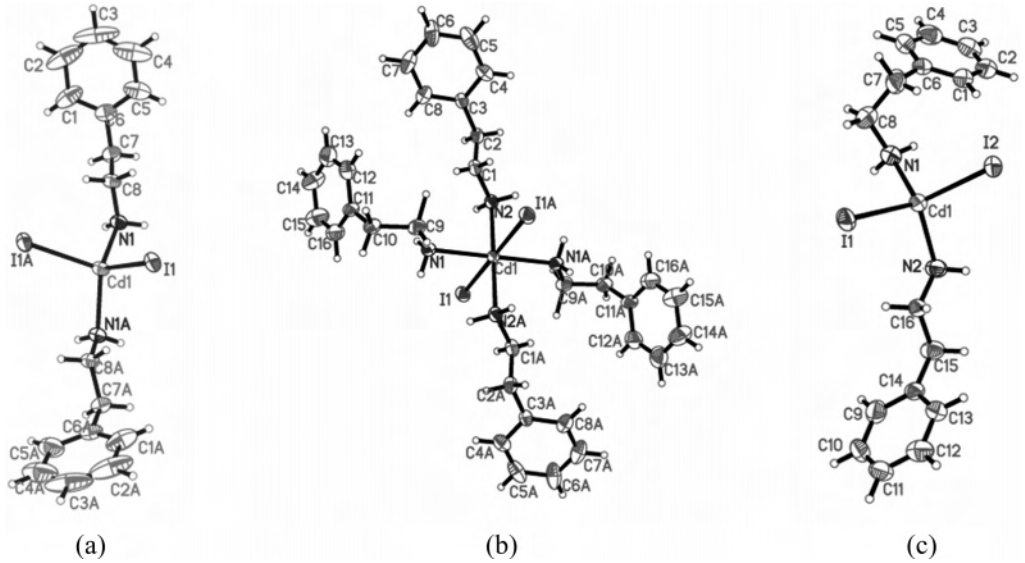

Figure 1. ORTEP drawings of compounds **1** (a) and **2** (b) and the $CdI_2(PEA)_2$ matrix of compound **3** (c) with 30% probability ellipsoids, showing the atomic numbering scheme. The doped CdS cannot be observed in the crystal structure due to the small amount.

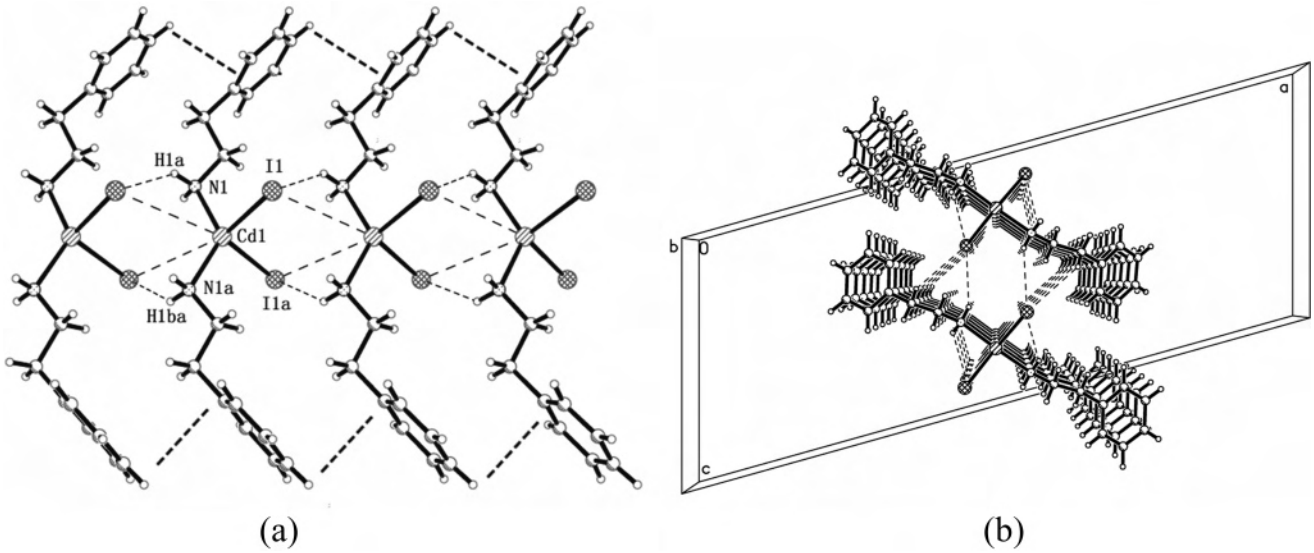

Figure 2. Hydrogen bondings and $\pi-\pi$ stacking in the crystal of compound **1** for (a) the single chain and (b) the adjacent chains. The thin dashed lines represent the hydrogen bondings, and the thick dashed lines represent the $\pi-\pi$ stacking interaction.

only $[CdI_2(pyridine)_4](pyridine)_2$ was reported with crystal structure, which contains enclathrated pyridine guest molecules. In contrast, compound **2** crystallizes without any enclathrated solvent molecules. PEA ligand coordinates to the cadmium atom through the amidogen, and the flexible ethylic group is conducive to reducing the steric hindrance and electron density at the metal center caused by the high coordination.[20] The bond lengths of Cd1−N1, Cd1−N2, and Cd1−I1 are 2.393, 2.372, and 3.030 Å, respectively, which are considerably longer than those in four-coordinated compound **1**. The Cd atom and four nitrogen atoms form a square-planar configuration, and the two iodine atoms are in the trans postion with I−Cd−I of 180.0°, indicating the existence of CdI_2N_4 octahedron.

These discrete CdI_2N_4 octahedra pack together by intermolecular hydrogen bondings of N−H···I and strong $\pi-\pi$ stacking interactions. As shown in Figure 3a, the hydrogen atoms linked with N1a and N2 involve in the hydrogen bondings with the same iodide atom of the neighboring molecule. However, the two hydrogen bondings are different in the bond length and angle. The N2−H8···I1 (x, $y + {}^1/_2$, $z - {}^1/_2$) hydrogen bonding with bond length of 2.939 Å is somewhat stronger than the N1a−H4b···I1 (x, $y + {}^1/_2$, $z - {}^1/_2$) with bond length of 3.009 Å. There is no intramolecular interaction between the aromatic rings, but strong $\pi-\pi$ stacking intermolecular interactions exist (3.105 Å, Figure 3b).

CdS-Doped $CdI_2(PEA)_2$ (3). Doping the metal sulfide nanoparticles such as CdS, PbS, ZnS, and SnS_2 to organic semiconductors have drawn much attention as the metal sulfides have excellent optical and electrical properties.[21−22]

(20) Strasdeit, H.; Saak, W.; Pohl, S.; Driessen, W. L.; Reedijk, J. *Inorg. Chem.* **1988**, *27*, 1557.

(21) Caseri, W. R. *Mater. Sci. Technol.* **2006**, *22*, 807.

(22) Aharon, E.; Kalina, M.; Frey, G. L. *J. Am. Chem. Soc.* **2006**, *128*, 15968.

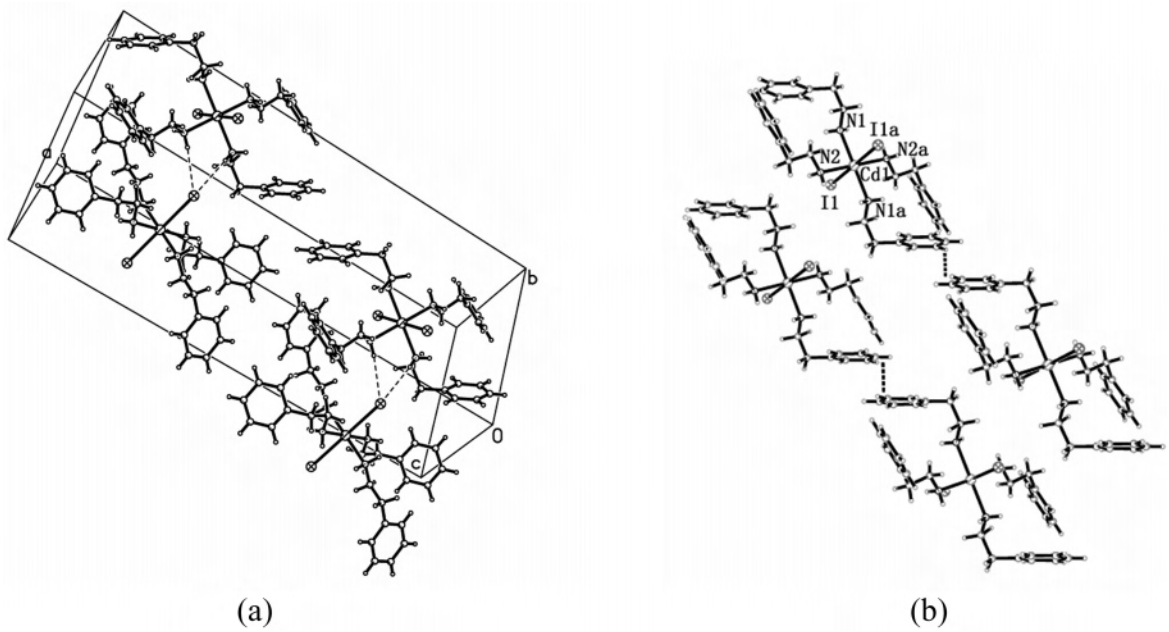

Figure 3. $\pi-\pi$ stacking (a) and hydrogen bondings (b) in the crystal of compound **2**. The thin dashed lines represent the hydrogen bonding, and the thick dashed lines represent the $\pi-\pi$ stacking interaction.

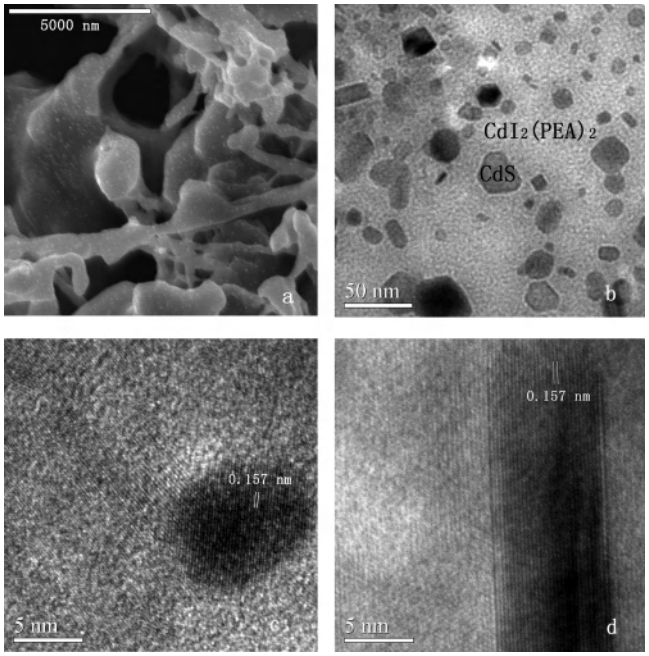

Figure 4. SEM (a) and HR-TEM (b−d) images of the CdS nanocrystals doped to the $CdI_2(PEA)_2$ matrix of compound **3**. Measured lattice spacings of images c and d correspond to (202) spacing in wurtzite CdS.

Herein, we have successfully prepared organic−inorganic hybrid $CdI_2(PEA)_2$ doped with nanocrystalline CdS. As described in the Experiment Section, the reaction was carried out at a relatively low temperature (the reflux temperature of methanol) and the reactants are safe and easily obtained. The trace amount of S is difficult to determine by elemental analysis, so we carried out X-ray fluorescence measurement, which gave the S amount of 0.2%. ICP-AES analysis revealed the absence of Na. The formula of compound **3** can be then expressed as $[CdI_2(PEA)_2](CdS)_{0.038}$. The doped CdS can be directly observed by the scanning electron microscopy and high-resolution transmission electron microscope (HR-TEM). As shown in Figure 4a, CdS nanoparticles uniformly disperse in the $CdI_2(PEA)_2$ matrix. Their diameter varies from 5 to 40 nm (Figure 4b). The lattice spacing of the CdS nanoparticles is 1.57 Å (Figure 4c,d), corresponding to the (2, 0, 2) plain spacing of wurtzite CdS.[23] The origin of the morphology of CdS nanoparticles may be related to the geometric structure of the $CdI_2(PEA)_2$ matrix, and the reaction of CdI_2 with Na_2S was confined into a nanoscale volume due to the linear structure of CdI_2 chains.[24]

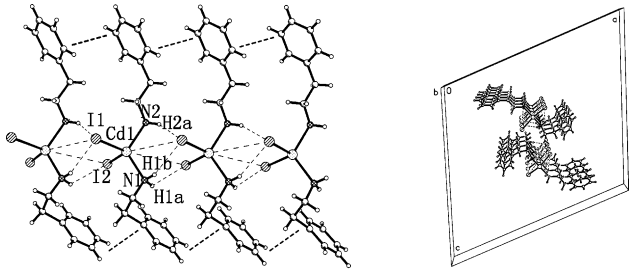

Figure 5. Hydrogen bondings and $\pi-\pi$ stacking in the $CdI_2(PEA)_2$ matrix of compound **3** for (a) the single chain and (b) the adjacent chains. The thin dashed lines represent the hydrogen bonding, and the thick dashed lines represent the $\pi-\pi$ stacking interaction.

Such a small amount of S (in the form of CdS) cannot exhibit in the powder diffraction analysis and single crystal analysis, which only gave the diffraction information of the $CdI_2(PEA)_2$ matrix. The main composition of compound **3** is still $CdI_2(PEA)_2$ which is similar to compound **1**. However, the crystal structure of the $CdI_2(PEA)_2$ matrix has been obviously changed by the incorporation of CdS nanoparticles. $CdI_2(PEA)_2$ in compound **3** belongs to the C_1 point group (while compound **1** belongs to C_{2v}), and one of the PEA

(23) Grun, M.; Hetterich, M.; Becker, U.; Giessen, H.; Klingshirn, C. *J. Cryst. Growth* **1994**, *141*, 68.
(24) Nie, Q.; Yuan, Q.; Chen, W.; Xu, Z. *J. Cryst. Growth* **2004**, *265*, 420.

ligands has a largely distorted configuration. Its amidogen folds down to the phenyl ring, leading to a smaller dihedral angle of 50.2° between the two phenyl rings of two PEA ligands than that in compound **1** (86.3°). The bond angle of N1−Cd1−N2 (116.2°) is smaller than that in compound **1**. The CdI_2N_2 tetrahedrons are also linearly linked together by intermolecular hydrogen bonding and $\pi-\pi$ stacking interaction. There are three different hydrogen bondings, as shown in Figure 5a. The hydrogen bondings of N1−H1b···I2 (x, $y-1$, z) and N1a−H1ba···I1 (x, $y-1$, z) turn out to be different and weaker, while in compound **1** they are identical. The bond lengths of H1a···I2 (x, $y+1$, z) and H2a···I1 (x, $y+1$, z) are 3.158 and 3.209 Å, respectively. Note the hydrogen bonding of N1−H1b···I1 (x, $y+1$, z) is a new one with a much smaller bond length of H1b···I1 (2.852 Å). The $\pi-\pi$ stacking interaction (3.345 Å) occurs between the phenyl/phenyl rings of the PEA ligands, and the interaction is somewhat stronger than that in compound **1**. However, the distance of adjacent Cd atoms (5.137 Å) in a single CdI_2 chain is fairly longer than that in compound **1** (4.846 Å). There is no interchain hydrogen bonding due to the increased distance between the nearest two CdI_2 chains.

It is amazing that such large variations in the overall crystal structure are caused by the small amount of dopant. Recently, a similar phenomenon was found in rhodamine 6G adsorbed on silver nanoparticles.[25] The angles between the xanthene plane and the phenyl substituent of rhodamine 6G are different when the molecules are adsorbed on two different adsorption sites. Enlightened by this work, we suggested a possible mechanism for the distorted configuration of CdI_2-$(PEA)_2$ matrix in compound **3**. As CdS has a smaller solubility than $CdI_2(PEA)_2$, it precipitated from the solution first and formed nanoparticles. Some $CdI_2(PEA)_2$ molecules may be adsorbed on the surface of the CdS nanoparticles and begin to crystallize. Because of the spatial hindrance of the CdS nanoparticles, the dihedral angle of two PEA groups turns out to be smaller than that in compound **1**.

Thermal Analysis. Thermal gravimetric analyses (TGA) were performed to determine the thermal stability of these compounds (as shown in Figure S2 of the Supporting Information). Compounds **1**−**3** thermally decompose by simple loss of the organic ligands, followed by sublimation of the metal halides. In compounds **1** and **3**, the PEA ligand is removed approximately at 120 °C, while in compound **2** the PEA ligand appears to be lost at a lower temperature of 91 °C due to the relatively longer bond length of Cd−N (2.372−2.393 Å). The cadmium iodide portion sublimes at approximately 400 °C for all the three compounds.

UV−Vis Spectroscopy. The solid-state diffuse reflectance spectra of compounds **1**−**3** were investigated at room temperature as shown in Figure 6. The band gap energy (E_g) value was determined by extrapolation from the linear portion of the absorption edge. The E_g values of compounds **1** and **2** are 4.36 and 4.45 eV, respectively. The larger E_g value of compound **2** compared with compound **1** may be due to the

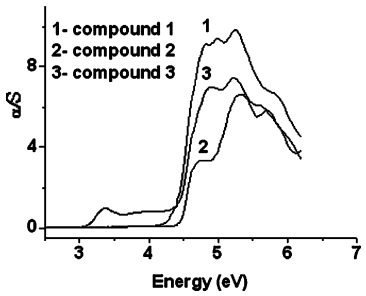

Figure 6. Solid-state diffuse reflectance spectra of compounds **1**−**3** at room temperature.

0D structure of CdI_2 in compound **2**, while compound **1** has a 1D structure of CdI_2 chains.[26] In the diffuse reflectance spectrum of compound **3**, there are two absorption edges from the onsets of the two linear increases with the values of 2.92 and 4.38 eV, which correspond to the E_g values of CdS[27] and the matrix of $CdI_2(PEA)_2$, respectively. Note that although the content of CdS is low, the absorption coefficient is as high as 1.6×10^5 cm^{-1}.[28] As a result, the signal of CdS nanoparticles in the solid-state diffuse reflectance spectrum is detectable.

Photoluminescence Spectroscopy. The photoluminescence spectra of compounds **1**−**3** were investigated in solid state at room temperature. As shown in Figure 7, compounds **1**−**3** exhibit blue, green, and orange emissions in the solid states at room temperature, respectively. Compound **1** has a strong emission band centered at 465 nm with an excitation band at 375 nm. Compound **2** exhibits a strong emission maximum at 512 nm ($\lambda_{ex} = 432$ nm) which is red-shifted by 47 nm compared with that of compound **1**. The difference in emission energies is most likely due to the iodide ligands acting as different roles (a bridging or terminal ligand) for **1** and **2**, respectively. In this context, the lower p-orbital energy for bridging iodide compared with the terminal one may be responsible for the blue shift in emission energies from **2** (512 nm) to **1** (465 nm). The emission spectrum of compound **3** features an overlapping band formed by two bands centered at 480 and 577 nm upon photoexcitation at 406 and 365 nm (Figure 7c). The emission band centered at 480 nm might be originated from the $CdI_2(PEA)_2$ matrix and the other emission band centered at 577 nm corresponds to the emission of CdS nanoparticles with the diameter varying from 5 to 40 nm in the solid state.[29]

We have also measured the time-resolved radiative decays of compounds **1**−**3** in solid state (as shown in Figure S3 of the Supporting Information). The radiative decay parameters including excitation and emission wavelengths, lifetimes, fractions, and average lifetimes are shown in Table 3. The decay curves of compounds **1** and **2**, and the $CdI_2(PEA)_2$ matrix of compound **3** are biexponetial, with lifetimes of

(25) Zhao, J.; Jensen, L.; Sung, J.; Zou, S.; Schatz, G. C.; Van, Duyne, R. P. *J. Am. Chem. Soc.* **2007**, *129*, 7647.

(26) Papavassiliou, G. C. *Prog. Solid State Chem.* **1997**, *25*, 125.

(27) (a) Xie, R.; Kolb, U.; Li, J.; Baschë, T.; Mews, A. *J. Am. Chem. Soc.* **2005**, *127*, 7480. (b) Tiwari, S.; Tiwari, S. *Cryst. Res. Technol.* **2006**, *41*, 78.

(28) Matsumoto, H.; Sakata, T.; Mori, H.; Yoneyama, H. *J. Phys. Chem.* **1996**, *100*, 13781.

(29) Wang, W.; Germanenko, I.; El-Shall, M. S. *Chem. Mater.* **2002**, *14*, 3028.

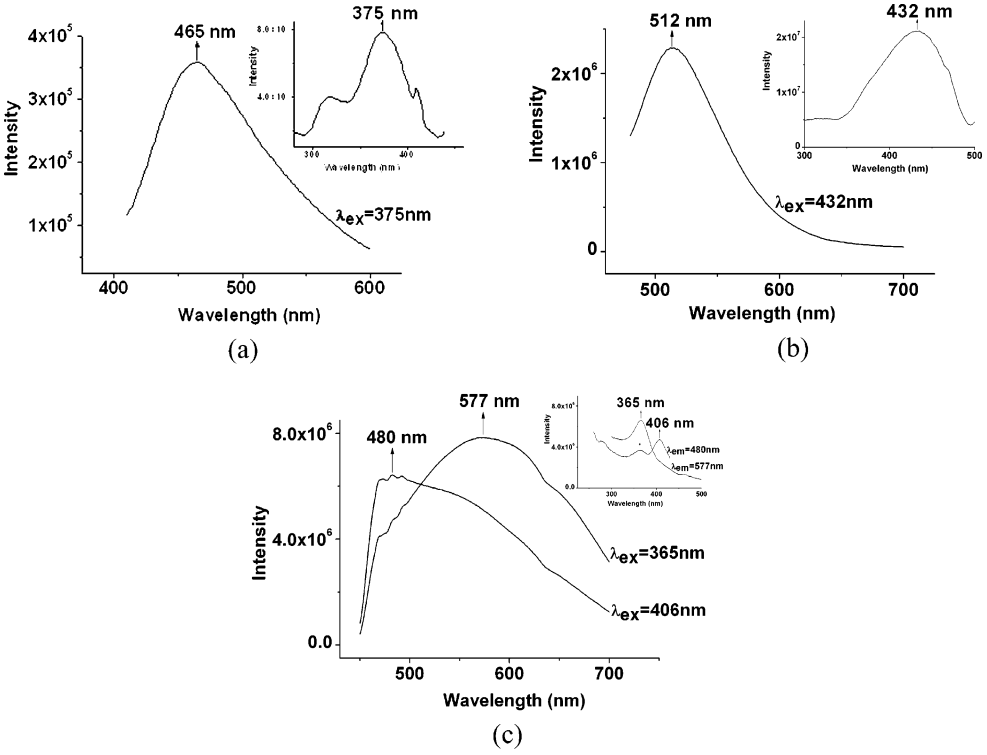

Figure 7. Photoluminescence spectra of compounds **1** (a), **2** (b), and **3** (c) in the solid state at room temperature Inset: excitation bands.

Table 3. Radiative Decay Parameters (Lifetimes, Fractions, and Average Lifetimes and Excitation and Emission Wavelengths) for Compounds **1**−**3**

compd	excitation wavelength/nm	emission wavelength/nm	τ_1/ns	τ_2/ns	α_1/%	α_2/%	τ_{av} [a]/ns[a]	χ [b]
1	375	465	1.445	6.096	43.68	56.32	4.06	1.073
2	432	512	1.704	4.353	75.94	24.06	2.34	1.008
3	406	450	1.508	5.759	66.53	33.47	2.93	1.111
	365	660	174.6		100			1.119

[a] $\tau_{av} = (\alpha_1\tau_1 + \alpha_2\tau_2)/(\alpha_1 + \alpha_2)$. [b]Goodness of fit parameter; $\chi^2 = 1$ for a good fit.

1.445 (43.68%) and 6.096 ns (56.32%) for compound **1**, 1.704 (75.94%) and 4.353 ns (24.06%) for compound **2**, and 1.508 (66.53%) and 5.759 ns (33.47%) for the $CdI_2(PEA)_2$ matrix of **3**. The average lifetimes τ_{av} [30] are obtained out of the two decay components for compounds **1**, **2**, and the $CdI_2(PEA)_2$ matrix of **3** and are determined to be 4.06, 2.34, and 2.93 ns, respectively, as shown in Table 3. The nanosecond scale of the decay times point out that all the above emission bands are from singlet excited states. Notice that the average lifetime of the $CdI_2(PEA)_2$ matrix of compound **3** is shorter than that of compound **1** due to the doped CdS nanoparticles. In addition, the emission at 660 nm from the doped CdS decays according to a single-exponential function and the lifetime is 174.6 ns, which is longer than the former reported lifetimes of undoped CdS (93−117 ns).[31] The changes of the lifetimes of the $CdI_2(PEA)_2$ matrix and CdS dopant in compound **3** strongly indicate the existence of energy transfer from the $CdI_2(PEA)_2$ matrix to the doped CdS nanoparticles.[32]

Typically, the emission mechanisms of cadmium halides with N-donor ligands are difficult to be attributed due to many factors.[33] However, the theoretical studies can give us a clear understanding of the photophysical properties of these compounds.[34] We performed theoretical studies of ground and excited electronic states of compounds **1**−**3**. For the calculated ground-state geometries, the electronic structure is examined in terms of the highest occupied molecular orbitals (HOMOs) and lowest unoccupied molecular orbitals (LUMOs). The nature of the low-lying excited states is then explored using TD-DFT approach to derive both absorption and emission spectra, which are compared with the above spectroscopic data.

Figure 8 illustrates the characteristics of the LUMOs and HOMOs of compounds **1** and **2** and the $CdI_2(PEA)_2$ matrix of **3**. Apparently, there is a large disparity in the distribution of the frontier orbitals between compounds **1** and **2**. For compound **1**, the electron densities of the HOMO are located on the iodine atoms, whereas those of the LUMO are distributed mainly on the cadmium atom, indicating that the lowest electronic transition might be attributed to iodide-to-

(30) Kishore, V. V. N. R.; Narasimhan, K. L.; Periasamy, N. *Phys. Chem. Chem. Phys.* **2003**, *5*, 1386.
(31) Lakowicz, J. R.; Gryczynski, I.; Gryczynski, Z.; Murphy, C. J. *J. Phys. Chem. B* **1999**, *103*, 7613.
(32) Jiu, T.; Li, Y.; Gan, H.; Li, Y.; Liu, H.; Wang, S.; Zhou, W.; Wang, C.; Li, X.; Liu, X.; Zhu, D. *Tetrahedron* **2007**, *63*, 232.
(33) Yu, J.; Ye, L.; Bi, M.; Hou, Q.; Zhang, X.; Xu, J. *Inorg. Chim. Acta* **2007**, *360*, 1987.
(34) Xiao, B.; Hou, H.; Fan, Y.; Tang, M. *Inorg. Chem. Commun.* **2007**, *10*, 376.

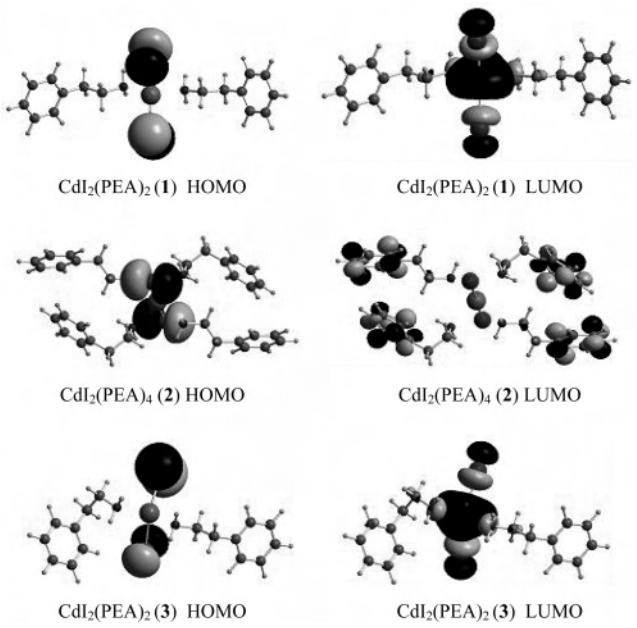

Figure 8. Surfaces of HOMOs and LUMOs in compounds **1** [$CdI_2(PEA)_2$], **2** [$CdI_2(PEA)_4$], and the matrix of **3** [$CdI_2(PEA)_2$] obtained at the B3LYP level. All the MO surfaces correspond to an isocontour value of $|\psi| = 0.03$ au.

cadmium charge transfer (XMCT).[35] In contrast, for compound **2**, although the electron densities of the HOMO are also distributed on the iodine atoms, those of the LUMO are located at the four phenyl rings of PEA ligands, suggesting that the lowest electronic transition might be dominated by halide-to-ligand charge transfer (XLCT).[9] The PEA ligand of compound **2** can be considered as a good electron acceptor for XLCT. We have also tried to use alkylamines (such as methylamine, ethylamine, and *n*-butylamine) instead of PEA as the ligands, but the products are optically inert. To further clarify the excited-state nature of these hybrid materials, we have also performed theoretical studies of $CdI_2(MA)_4$ (MA = methylamine). For $CdI_2(MA)_4$, the electron densities of the HOMO are located on the iodine atoms and those of the LUMO mainly on the cadmium atom (as shown in Figure S4), indicating the XMCT mechanism. Compared with PEA, methylamine is a weak acceptor and not suitable for the XLCT mechanism which exists in $CdI_2(PEA)_4$. Although the $CdI_2(PEA)_2$ matrix of compound **3** has some distortion in one PEA ligand compared with compound **1**, the electron densities of the HOMO and LUMO exhibit almost the same distribution as that in compound **1**, explaining that the high-energy emission band of compound **3** might also result from the XMCT of the $CdI_2(PEA)_2$ matrix.

TDDFT calculations are employed to examine the low-lying singlet excited states of compounds **1** and **2**, and the $CdI_2(PEA)_2$ matrix of compound **3**. Selected three singlet excited states with the greatest oscillator strengths are displayed in Table S2 of the Supporting Information. The energy of each excited state is vertical excitation energy in electronvolts from the ground state. The excited-state electronic structures are best described in terms of multiconfigurations, wherein a linear combination of several occupied-to-virtual MO excitations comprises a given optical absorption.[36] Assignment of the characteristics of each excited state was based on the compositions of the occupied and virtual MOs of the dominant configurations for that excited state. For compound **1** and the $CdI_2(PEA)_2$ matrix of compound **3**, all of the selected excited states are designated to be XMCT, since all the involved occupied orbitals are iodine-based and all the involved virtual orbitals are metal-based.[37] For compound **2**, although the first singlet excited state corresponding to the transition from HOMO to LUMO is forbidden ($a_u \rightarrow a_u$) due to the spatial symmetry selection rules,[38] the other selected excited states with greatest oscillator strengths are designated to be XLCT, because all of the involved occupied orbitals are iodine-based but all the involved virtual orbitals are PEA-based π^*.[39] That is consistent with the deduction from the electronic structures of ground states. The calculated lowest energy absorption peaks are 293 nm (4.24 eV) for compound **1**, 274 nm (4.53 eV) for compound **2**, and 292 nm (4.25 eV) for the $CdI_2(PEA)_2$ matrix of compound **3**, which are in good agreement with the experimental energy gaps for these three materials from absorption spectra.

Conclusion

This paper reports the synthesis and properties of three kinds of organic−inorganic hybrid materials based on CdI_2 and PEA (phenethylamine). By controlling the stoichiometric ratio used, $CdI_2(PEA)_2$ (**1**) and $CdI_2(PEA)_4$ (**2**) with quite different structures were successfully synthesized. By introducing a small amount of Na_2S to the reaction mixture, CdS nanoparticles can be easily doped to the $CdI_2(PEA)_2$ matrix to obtain a new compound **3** with the formula of $[CdI_2(PEA)_2](CdS)_{0.038}$. The existence of CdS nanoparticles give an amazing effect on the crystal structure of the $CdI_2(PEA)_2$ matrix of compound **3**. Compounds **1**−**3** display bright blue, green, and orange emissions in the solid state at room temperature, respectively. The molecular orbital calculations make it clear that the emission of compound **1** and the $CdI_2(PEA)_2$ matrix of compound **3** are originated from a singlet "CdI_2-centered" halide-to-metal charge transfer (XMCT) excited state, while the emission of compound **2** is designated to a halide-to-ligand charge transfer (XLCT). It is worthwhile to note that the complex emission of compound **3** might be ascribed to a mixture of the $CdI_2(PEA)_2$ matrix and the doped CdS nanopaticles. Our work proves that the structures and photoelectronic properties of the organic−inorganic hybrid materials can be finely tuned by controlling the stoichiometric ratio used and doping inorganic semiconductor nanoparticles. What is more, the synthesis of compound **3** provides a new and simple method to prepare CdS nanoparticles.

(35) Wu, T.; Li, D.; Ng, S. W. *CrystEngComm* **2005**, *7*, 514.
(36) Nelson, S. F.; Weaver, M. N.; Yamazaki, D.; Komatsu, K.; Rathore, R.; Bally, T. *J. Phys. Chem. A* **2007**, *111*, 1667.
(37) Bardaji, M.; Calhorda, M. J.; Costa, P. J.; Jones, P. G.; Laguna, A.; Pérez, M. R.; Villacampa, M. D. *Inorg. Chem.* **2006**, *45*, 1059.
(38) Steiner, E.; Fowler, P. W. *J. Phys. Chem. A* **2001**, *105*, 9553.
(39) Zhao, Q.; Liu, S.; Shi, M.; Wang, C.; Yu, M.; Li, L.; Li, F.; Yi, T.; Huang, C. *Inorg. Chem.* **2006**, *45*, 6152.

Acknowledgment. This work was supported by the National Natural Science Foundation of China (Grant Nos. 50433020 and 50403001), the National Basic Research Program of China (Grant No. 2006CB806200), and the National Science Foundation of the United States (Grant CHE-06-16849).

Supporting Information Available: Listings of X-ray crystallographic data in CIF format for compounds **1**−**3**, packing of the inorganic frameworks of compounds **1** and **3**, TGA curves of compounds **1**−**3**, time-resolved radiative decays of compounds **1**−**3**, theoretical calculation results of $CdI_2(MA)_4$ (MA = methylamine), hydrogen bonding of compounds **1**−**3**, and TDDFT calculation results of compounds **1**−**3**. This material is available free of charge via the Internet at http://pubs.acs.org.

IC7007304